BIOMOLECULES & THERAPEUTICS

Original Article
Biomol Ther 26(5), 494-502 (2018)

Imidazole Antifungal Drugs Inhibit the Cell Proliferation and Invasion of Human Breast Cancer Cells

Sung Hun Bae[1], Ju Ho Park[1], Hyeon Gyeom Choi[2], Hyesook Kim[3] and So Hee Kim[1,*]

[1]College of Pharmacy and Research Institute of Pharmaceutical Science and Technology, Ajou University, Suwon 16499,
[2]Department of Systems Biotechnology, Konkuk Institute of Technology (KIT), Konkuk University, Seoul 05029, Republic of Korea
[3]Detroit R&D Inc, Detroit, MI 48105, USA

Abstract

Breast cancer is currently the most prevalent cancer in women, and its incidence increases every year. Azole antifungal drugs were recently found to have antitumor efficacy in several cancer types. They contain an imidazole (clotrimazole and ketoconazole) or a triazole (fluconazole and itraconazole) ring. Using human breast adenocarcinoma cells (MCF-7 and MDA-MB-231), we evaluated the effects of azole drugs on cell proliferation, apoptosis, cell cycle, migration, and invasion, and investigated the underlying mechanisms. Clotrimazole and ketoconazole inhibited the proliferation of both cell lines while fluconazole and itraconazole did not. In addition, clotrimazole and ketoconazole inhibited the motility of MDA-MB-231 cells and induced G_1-phase arrest in MCF-7 and MDA-MB-231 cells, as determined by cell cycle analysis and immunoblot data. Moreover, Transwell invasion and gelatin zymography assays revealed that clotrimazole and ketoconazole suppressed invasiveness through the inhibition of matrix metalloproteinase 9 in MDA-MB-231 cells, although no significant changes in invasiveness were observed in MCF-7 cells. There were no significant changes in any of the observed parameters with fluconazole or itraconazole treatment in either breast cancer cell line. Taken together, imidazole antifungal drugs showed strong antitumor activity in breast cancer cells through induction of apoptosis and G_1 arrest in both MCF-7 and MDA-MB-231 cells and suppression of invasiveness via matrix metalloproteinase 9 inhibition in MDA-MB-231 cells. Imidazole drugs have well-established pharmacokinetic profiles and known toxicity, which can make these generic drugs strong candidates for repositioning as antitumor therapies.

Key Words: Breast cancer, Imidazole, Cell proliferation, Apoptosis, Invasion, MMP9

INTRODUCTION

Breast cancer is the second most prevalent cancer worldwide. It accounts for 25% of all cancers in women (Bray *et al*., 2013) and is the primary cause of cancer death among women (Ferlay *et al*., 2013). In recent years, breast cancer incidence has risen sharply, particularly in advanced countries where the rate of breast cancer diagnoses is greater than that in developing ones. One of the main characteristics of breast cancer cells is their ability to invade nearby tissue. These mobile cancer cells can reach lymph nodes and from there, adhere to other organs such as bones, the liver, or the lungs, leading to metastases that are the primary cause of breast cancer-related death (Steeg, 2006). Therefore, it is critical to detect and treat breast cancer early, before metastases can develop.

Azole compounds are typically used as antifungal drugs. They inhibit the ergosterol biosynthesis pathway through suppression of the enzyme lanosterol 14-α-demethylase, a cytochrome P450 (CYP) enzyme; the consequent lack of ergosterol causes membrane abnormalities (Tripathi, 2013). Structurally, azole antifungal drugs consist of an imidazole [clotrimazole (CTZ) and ketoconazole (KCZ)] or a triazole [fluconazole (FCZ) and itraconazole (ICZ)] ring (Fig. 1). Triazole compounds are less toxic and produce fewer side effects than imidazole compounds since triazole compounds have a lower affinity for CYP and lower inhibitory effects on sterol synthesis (Tripathi, 2013; Tsubamoto *et al*., 2017).

Although azole drugs are primarily used as antifungal agents, recently, some azole drugs have shown antitumor activity. For example, CTZ was reported to inhibit tumor growth and suppress metabolic enzymes in lung carcinoma and co-

Open Access **https://doi.org/10.4062/biomolther.2018.042**

Received Mar 5, 2018 **Revised** Jun 22, 2018 **Accepted** Jul 17, 2018
Published Online Aug 10, 2018

***Corresponding Author**
E-mail: shkim67@ajou.ac.kr
Tel: +82-31-219-3451, Fax: +82-31-219-3435

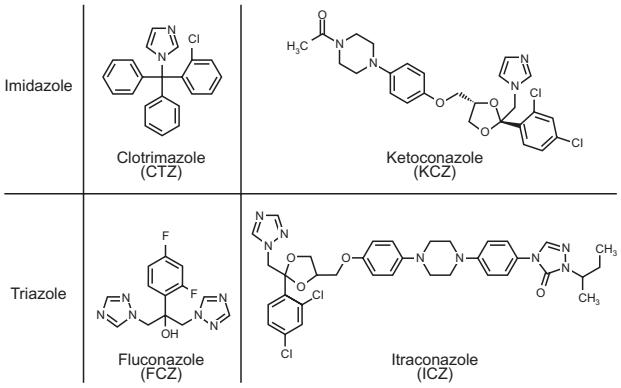

Fig. 1. Structures of imidazole [clotrimazole (CTZ) and ketoconazole (KCZ)] and triazole [fluconazole (FCZ) and itraconazole (ICZ)] compounds.

lon adenocarcinoma cells (Kadavakollu *et al*., 2014). Similarly, KCZ was reported to block multiple steps in androgen synthesis through the inhibition of CYP17A1 in castration-resistant prostate cancer patients being treated with dutasteride for benign prostatic hyperplasia (Taplin *et al*., 2009; Vasaitis *et al*, 2011). ICZ showed selective inhibitory activity against tumor-associated angiogenesis in non-small cell lung cancer (Aftab *et al*., 2011) and antitumor efficacy in prostate cancer patients (Antonarakis *et al*., 2013).

Most of these studies were clinical trials of azole antifungal drugs in major carcinomas including lung, prostate, and colon cancers. Thus, the comparative effects of different azole compounds on cancer cell proliferation and apoptosis have not been extensively studied. To address this issue, we evaluated the effects of four major azole compounds (two imidazole and two triazole compounds) on cell proliferation, apoptosis, migration, and invasion into other tissues. We then investigated the underlying mechanism of these drugs using human breast adenocarcinoma cells.

MATERIALS AND METHODS

Materials

CTZ, KCZ, FCZ, ICZ, dimethylsulfoxide (DMSO), 3-(4,5-dimethylthiazol-2-yl)-2-5-diphenyltetrazolium bromide (MTT), mitomycin C, Matrigel, and collagen were obtained from Sigma-Aldrich (St. Louis, MO, USA). Polycarbonate membrane insert (pore size 8 μm) was purchased from Corning (Middleland, MI, USA). Gelatin was obtained from Wako (Tokyo, Japan). The primary antibodies against p53, p27, p21, poly ADP ribose polymerase (PARP), cyclin dependent kinase (CDK) 2, CDK4, cleaved caspase3, Bcl2, and Bax were purchased from Cell Signaling Technology (Beverly, MA, USA). Cyclin D1, cyclin E1, and glyceraldehyde 3-phosphate dehydrogenase (GAPDH) were obtained from Sigma-Aldrich. Secondary rabbit and mouse antibodies were purchased from Bio-Rad (Hercules, CA, USA). All other materials were of reagent grade and used without further purification.

Cell lines

MCF-7 and MDA-MB-231 human breast adenocarcinoma cell lines were purchased from American Type Culture Collection (ATCC, Manassas, VA, USA). Both cell lines were maintained in RPMI 1640 (with L-glutamine and sodium bicarbonate), supplemented with 10% (v/v) fetal bovine serum (FBS) and 1% (v/v) penicillin and streptomycin (Invitrogen, Carlsbad, CA, USA). Cells were incubated at 37°C in 5% CO_2 atmosphere (Tran *et al*., 2017).

Cell proliferation assay

To evaluate the effect of azole drugs on cell proliferation, cells were plated into a 96-well plate at the appropriate density (5–10×10^3 cells/100 μL medium), as determined based on growth characteristics. After overnight incubation, the cells were treated with various concentrations (1, 8, 10, 16, 20, 32, 50, 64, 100, and 128 μM) of each drug, and left to incubate for 72 h. Thereafter, the medium was removed and 100 μL diluted MTT (0.5% MTT stock diluted 1:10 with medium) was added to each well for 2 h at 37°C. Subsequently, the content of each well was diluted with 100 μL DMSO to solubilize the purple formazan crystals. The optical density (OD) was measured at 540 nm with a Biotek enzyme-linked immunosorbent assay (ELISA) reader (Fisher Scientific, Norcross, GA, USA) (Tran *et al*., 2017).

Wound healing assay

MCF-7 and MDA-MB-231 cells were seeded into 6-well plates to create a confluent monolayer. After overnight incubation, mitomycin C was treated with the final concentration of 25 μg/mL, and the cells were left for 30 min at 37°C. The medium was then suctioned and a straight line was scratched in the middle of the cell monolayer with a pipette tip. To remove cellular debris, the cells were washed with 1 mL of phosphate buffered saline (PBS), placed in 2 mL of medium and then treated with 100 μM of CTZ, KCZ, FCZ, or ICZ. After 8-h incubation, the widths of the scratched line were measured and compared to that at 0 h (Mander *et al*., 2018).

Apoptosis assay

In order to evaluate whether the azole compounds induce apoptosis in breast cancer cells, MCF-7 and MDA-MB-231 cells were seeded into 6-well plates. After overnight incubation, the cells were treated with 50 μM of each azole antifungal drug for 24 h. Apoptosis was measured using an annexin V-FITC/PI kit (Abcam, Cambridge, UK) according to the manufacturer's instruction. Briefly, control and azole antifungal drug-treated breast cancer cells were trypsinized, collected via centrifugation and washed once with PBS. Cells were then re-colored with 5 μL annexin V- FITC and 10 μL propidium iodide (PI) for 15 min at room temperature, analyzed using a FACS Calibur flow cytometer, and identified using Cell Quest software (Becton-Dickinson, San Jose, CA, USA) (Zhao *et al*., 2018).

Flow cytometry

In order to assess cell cycle progression, MCF-7 and MDA-MB-231 cells were plated onto 60 mm dishes. After incubation overnight, cells were treated with 50 μM of CTZ, KCZ, FCZ, or ICZ for 24 h. Cells were then trypsinized and centrifuged at 500× *g* and 4°C for 5 min, and fixed with 70% ethanol at 4°C, followed by the addition of 1 mL PI solution (final concentration, 50 μg/mL) containing 200 μg/mL RNase A, for 30 min in the dark (Fujita *et al*., 2016). Flow cytometry was then performed using FACS Calibur and analyzed using Cell Quest

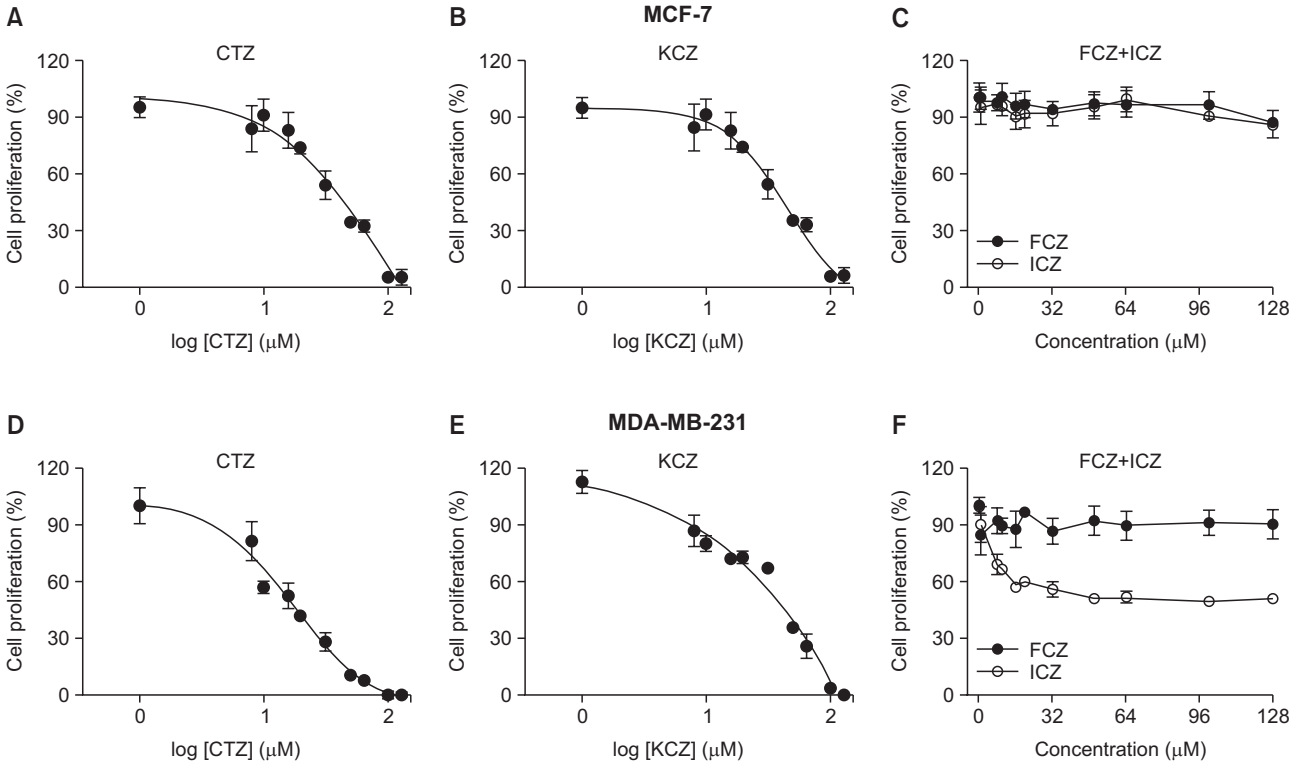

Fig. 2. Anti-proliferative effects of azole compounds on the human breast adenocarcinoma cell lines, MCF-7 and MDA-MB-231. MCF-7 cells were treated with CTZ (A), KCZ (B) and FCZ and ICZ (C) for 72 h. MDA-MB-231 cells were also treated with CTZ (D), KCZ (E) and FCZ and ICZ (F) for 72 h. This experiment was performed three times and data are expressed as mean ± standard deviation (n=3). CTZ, clotrimazole; KCZ, ketoconazole; FCZ, fluconazole; ICZ, itraconazole.

software (Becton-Dickinson). Red fluorescence, measured at 585/542 nm, indicative of PI uptake by damaged cells, was measured using logarithmic amplification and electronic compensation for spectral overlap (Lim *et al*., 2015).

Protein extraction and immunoblot analysis

MCF-7 and MDA-MB-231 cells were seeded in 60 mm dishes. After incubation overnight, the cells were treated with 50 μM of CTZ, KCZ, FCZ, or ICZ for 24 h, washed with cold PBS twice, and supplemented with 200 μL lysis buffer containing protease inhibitor cocktail (Sigma-Aldrich) in a cold room (4°C) for 30 min. Cell lysates were then at 4°C and 12,000 rpm for 20 min. The supernatant was collected and the protein concentration was measured using a bicinchoninic acid (BCA) assay. For immunoblot analysis, protein samples (20-40 μg of protein per lane) were resolved via sodium dodecyl sulfate polyacrylamide gel electrophoresis (SDS-PAGE) on a gel (10%) and transferred to nitrocellulose for 1 h. For immunodetection, blots were incubated overnight with the appropriate diluted primary antibody (1:1,000) in 5% bovine serum albumin (BSA) and tris-buffered saline (TBS) with 0.1% tween 20 (TBS-T) at 4°C with gentle shaking, followed by incubation with a secondary antibody conjugated to horseradish peroxidase for 1 h at room temperature. Protein expression was detected via enhanced chemiluminescence (Detroit R & D, Detroit, MI, USA) using an ImageQuant LAS-4000 mini (GE Healthcare Life Sciences, Piscataway, NJ, USA). The band density was quantified using ImageJ 1.45s software. GAPDH was used as an internal standard (Zhao *et al*., 2018).

Cell invasion assay

The outer membrane of a polycarbonate membrane insert (pore size 8 μm) was coated with 0.5 mg/mL collagen and the insert with 10 μL Matrigel diluted with 20 μL PBS. MCF-7 and MDA-MB-231 cells were seeded in the insert (7×10^4 cells/each insert) and treated with 50 μM of CTZ, KCZ, FCZ, or ICZ in RPMI 1640 medium without FBS. After incubation for 48 h at 37°C, the inserts were stained with 500 μL cell stain solution for 20 min and washed several times with distilled water. The inserts were then air-dried and dissolved in 200 μL methanol, and 100 μL dye/solute mixture was transferred to a 96-well plate. The invasion ability of the cells was detected by measuring the absorbance at 540 nm using a Biotek ELISA reader (Fisher Scientific) (Mander *et al*., 2018).

Gelatin zymography assay

MCF-7 and MDA-MB-231 cells were seeded when they were approximately 80% confluent in 60-mm dishes and incubated overnight at 37°C. The cells were washed with PBS to remove the FBS. Cells were then incubated in serum-free medium with 50 μM of CTZ, KCZ, FCZ, or ICZ at 37°C for 48 h. To analyze matrix metalloproteinase (MMP) activity such as MMP2 and MMP9, the medium was harvested, concentrated using a speed vac (Eppendorf, Hicksville, NY, USA), and the protein concentration was measured via BCA assay. Protein (100 μg) was loaded in 10% SDS-PAGE containing 0.1%

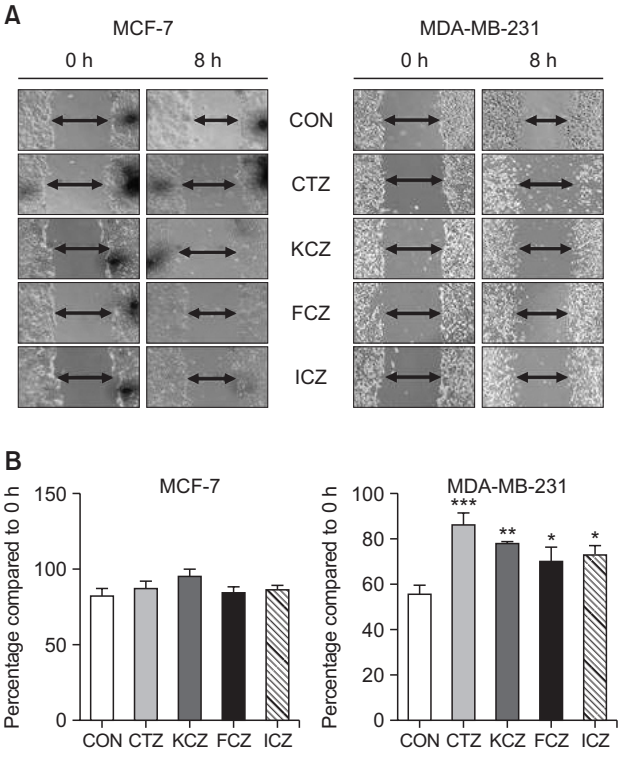

Fig. 3. Effect of azole compounds on wound healing. Wound healing assays of imidazole compounds [clotrimazole (CTZ) and ketoconazole (KCZ)] and triazole [fluconazole (FCZ) and itraconazole (ICZ)] compounds were performed in MCF-7 and MDA-MB-231 cells. (A) Representative photographs of MCF-7 and MDA-MB-231 cells at 0 h and 8 h after treatment of each compound (100 μM). (B) Wound percentages were calculated by dividing the width at 8 h by the width at 0 h for each treatment (100 μM). This experiment was performed three times and data are expressed as mean ± standard deviation (n=3). *p<0.05, **p<0.01, ***p<0.001.

gelatin. The gel was washed twice alternately with renaturing buffer (2.5% Triton X-100, v/v) and distilled water and then incubated with developing buffer (50 mM Tris-Base, 150 mM NaCl, 1 μM $ZnCl_2$, 0.02% NaN_3, 5 mM $CaCl_2$•$2H_2O$, pH 7.5) at 37°C for 48 h. The gel was stained with 0.5% Coomassie blue for 1 h and destained with destaining buffer (5% acetic acid in 10% methanol, v/v). The band density was measured using ImageJ 1.45s software (National Institutes of Health [NIH], Bethesda, MD, USA) (Mander *et al*., 2018).

Xenograft tumor tissue fractionation

Female nude mice [6 weeks old; BALB/c-nu (nu/nu)] were purchased from Orientbio (Seongnam, Korea) and maintained in clean conditions. This study was conducted in accordance with the Guide for the Care and Use of Experimental Animals, with the approval from the Laboratory Animal Research Center of Ajou University Medical Center, Institutional Animal Care and Use Committee (IACUC No. 2015-0026). MDA-MB-231 cells were subcutaneously injected into the mice (2×10^6 in 200 μL) and tumors were allowed to develop for 30 days until they reached 40 mm^3, at which point treatment was initiated. Mice were randomly divided into 5 groups [control (CON), CTZ, KCZ, FCZ, ICZ, each n=5-8]. The mice in each azole drug group (100 mg/kg of body weight) were injected with 0.2 mL of

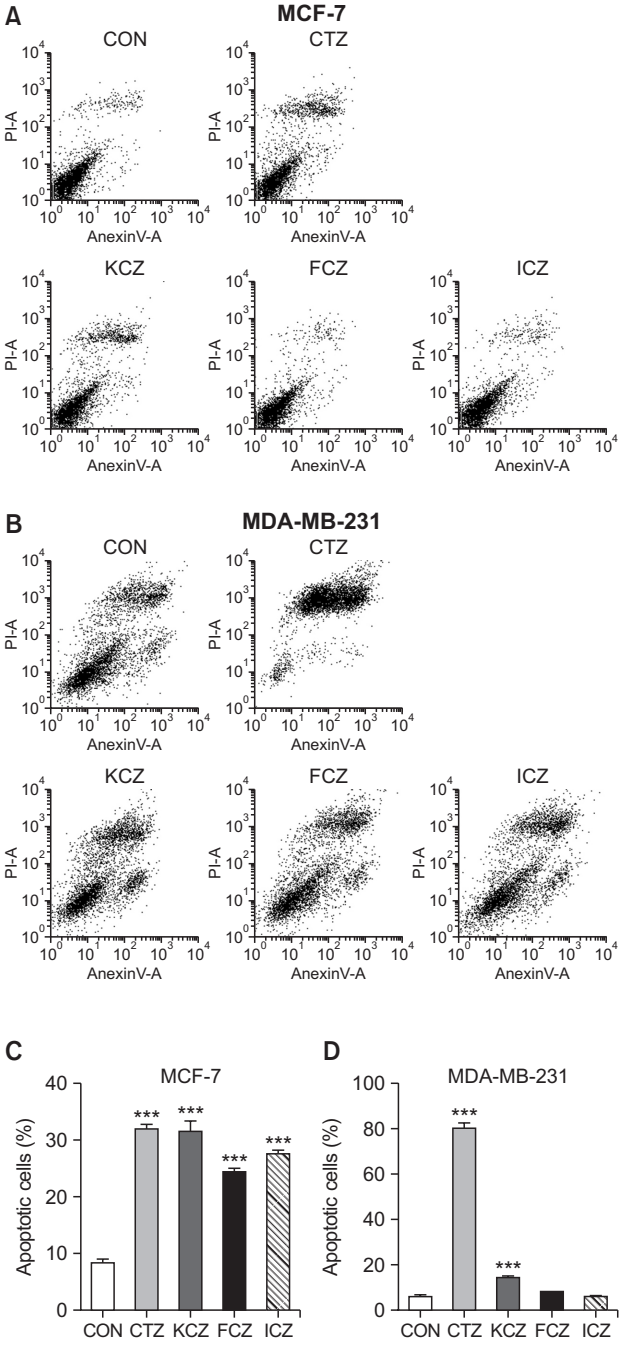

Fig. 4. Azole antifungal drugs induced apoptosis in human breast cancer cell lines. MCF-7 and MDA-MB-231 cells were treated with dimethylsulfoxide (CON) and 50 μM of imidazole [clotrimazole (CTZ) or ketoconazole (KCZ)] or triazole [fluconazole (FCZ) or itraconazole (ICZ)] compounds for 24 h. Apoptosis was measured using an annexin V-FITC/PI kit. Histograms of MCF-7 (A) and MDA-MB-231 (B) cells were obtained from FACS Calibur flow cytometer. Bar graphs were obtained by analyzing apoptotic cells of MCF-7 (C) and MDA-MB-231 (D) cells using Cell Quest software (Becton-Dickinson). This experiment was performed three times and data are expressed as mean ± standard deviation (n=3). ***p<0.001.

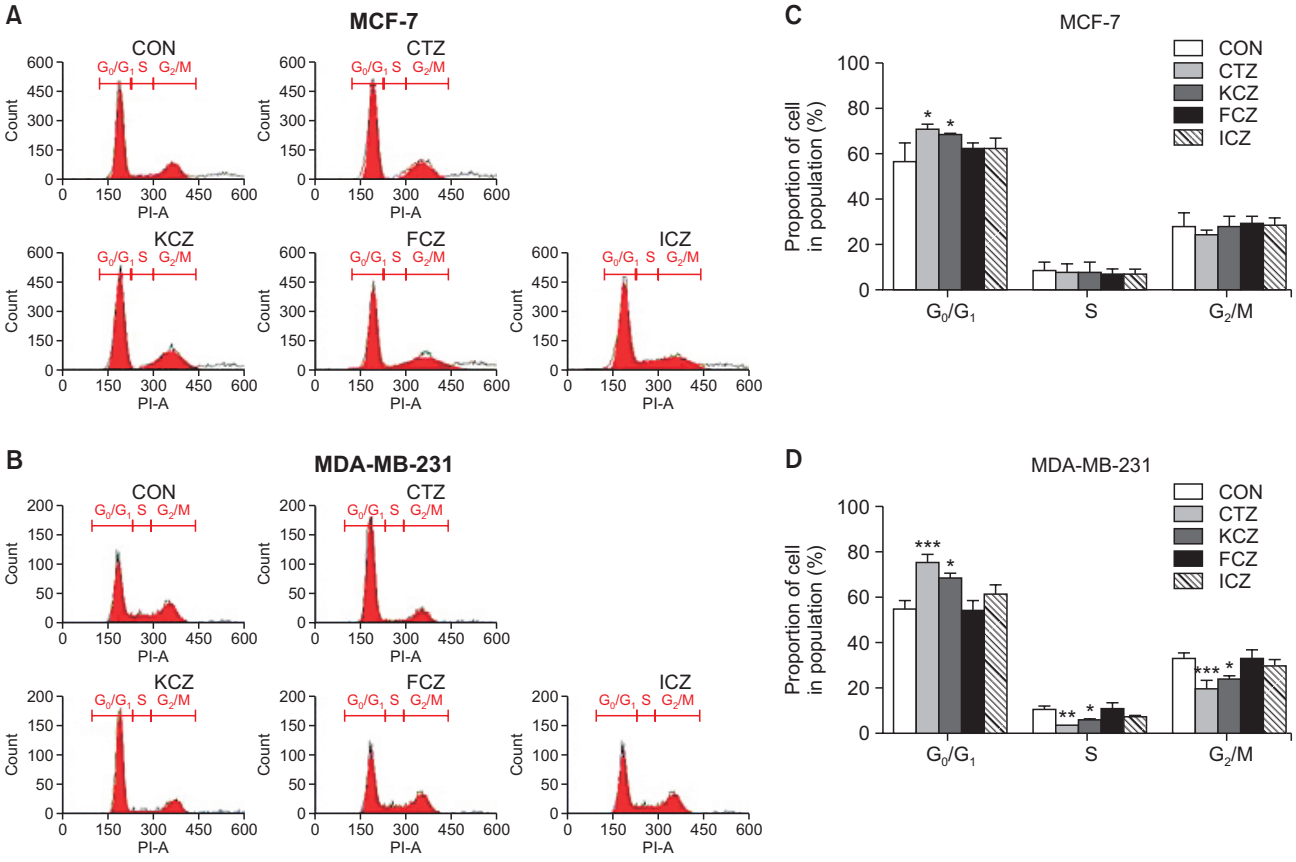

Fig. 5. Relative DNA content according to cell cycle stage. Cell cycle progression was analyzed via flow cytometry with propidium iodide (PI) staining using MCF-7 and MDA-MB-231 cells treated with 50 μM imidazole [clotrimazole (CTZ) or ketoconazole (KCZ)] or triazole [fluconazole (FCZ) or itraconazole (ICZ)] compounds for 24 h. Histograms were obtained from MCF-7 (A) and MDA-MB-231 (B) cells via flow cytometry. Bar graphs were obtained by analyzing the relative cell cycle phase distribution of MCF-7 (C) and MDA-MB-231 (D) cells. The data were analyzed using Cell Quest software (Becton-Dickinson). This experiment was performed three times and data are expressed as means ± standard deviation of triplicate determinations. **p*<0.05, ***p*<0.01, ****p*<0.001.

the drug intraperitoneally every other day. The control group was treated with an equal volume of vehicle. After transplantation, the tumor size was measured using calipers, and the tumor volume was estimated according to the following formula: tumor volume (mm^3)=L×W^2/2, where L is the length and W is the width (Li *et al*., 2017). Tumor-bearing mice were killed after 60 days. Xenograft tumors were harvested and homogenized with radioimmunoprecipitation assay (RIPA) lysis buffer (150 mM NaCl, 1% NP40, 0.5% deoxycholate, 50 mM Tris-HCl at pH 8, 0.1% SDS, 10% glycerol, 5 mM EDTA, 20 mM NaF, and 1 mM Na_3VO_4). The total homogenate was centrifuged at 12,000 rpm for 20 min at 4°C. The supernatant was collected and used for immunoblot analysis.

Statistical analysis

Data are presented as the mean ± standard deviation (SD). Statistical analysis was performed using Prism 5 (GraphPad, La Jolla, CA, USA). Data were compared using unpaired *t*-test between two groups or one-way analysis of variance (ANOVA) followed by Dunnett's *post hoc* test among more than three groups. *p* values of <0.05 were considered statistically significant (Cook *et al*., 2012).

RESULTS

Effects on cell proliferation

The anti-proliferative effects of azole compounds on human breast adenocarcinoma MCF-7 and MDA-MB-231 cells are shown in Fig. 2. The imidazole compounds CTZ and KCZ exhibited a greater anti-proliferative activity against MCF-7 (Fig. 2A, 2B) and MDA-MB-231 (Fig. 2D, 2E) cells than the triazole compounds, FCZ and ICZ (Fig. 2C, 2F); this effect was concentration-dependent. The concentrations of CTZ and KCZ that inhibited cell growth by 50% (IC_{50}) were 21.0 and 35.1 μM, respectively, for MCF-7 cells and 23.1 and 41.8 μM, respectively, for MDA-MB-231 cells. However, the anti-proliferative effect of FCZ was almost negligible in both cell lines while ICZ inhibited the proliferation of MDA-MB-231 cells by 50% at 50 μM (Fig. 2F) and maintained this inhibition level at higher concentrations. IC_{50} values were not measured for both FCZ and ICZ in both breast cancer cells.

Wound healing assay

Next, we examined the effect of azole compounds on the motility of cancer cells via a wound healing assay. There were no significant differences in MCF-7 cells after treatment with

either imidazole or triazole compounds, except for KCZ (Fig. 3). The wound healing rate of untreated (CON) and KCZ-treated cells after 8 h was 17.6% and 5.3%, respectively. In contrast, the wound healing rate of MDA-MB-231 cells was significantly reduced by treatment with CTZ and KCZ. The wound healing rate of CON-, CTZ-, and KCZ-treated cells after 8 h was 44.2%, 13.6%, and 21.8%, respectively, while that of FCZ- and ICZ-treated cells after 8 h was 29.8% and 27.1%, respectively (Fig. 3).

Apoptosis assay

To examine whether azole antifungal drugs induced apoptosis in MCF-7 and MDA-MB-231 cells, cells were treated with each drug at a concentration of 50 μM for 24 h. As shown in Fig. 4, the imidazole drugs (CTZ and KCZ) significantly increased apoptosis in both MCF-7 and MDA-MB-231 cells, while the triazole drugs only increased apoptosis in MCF-7 cells.

Flow cytometry

We performed flow cytometry to assess the effect of antifungal agents on cell cycle progression in MCF-7 and MDA-MB-231 cells (Fig. 5). CTZ and KCZ induced G_1 phase arrest in both MCF-7 and MDA-MB-231 cells (Fig. 5). In MCF-7 cells, the proportion of G_1 phase cells significantly increased after CTZ and KCZ treatment by 25.0% and 20.1%, respectively. In MDA-MB-231 cells, the proportion of G_1 phase cells also significantly increased after treatment with CTZ and KCZ by 36.3% and 23.7%, respectively, and the proportion of S and G_2/M phase cells significantly decreased. Treatment with FCZ and ICZ did not alter the proportion of cells in each phase in either breast cancer cell line.

Immunoblot analysis

Next, we evaluated protein expression using immunoblot analysis. Treatment with CTZ induced PARP cleavage in both MCF-7 and MDA-MB-231 cells, while KCZ induced PARP cleavage only in MDA-MB-231 cells (Fig. 6A). Cleaved caspase-3, another marker of apoptosis, was also detected after CTZ treatment in both breast cancer cell lines (Fig. 6A). The expression of Bcl-2, an antiapoptotic marker, was lower in both MCF-7 and MDA-MB-231 cells treated with the imidazoles (CTZ and KCZ) than in untreated cells (Fig. 6A). In contrast, all azole compounds increased Bax expression in both breast cancer cell lines (Fig. 6A).

We examined the expression of proteins involved in the G_1 phase cell cycle in MCF-7 and MDA-MB-231 cells after treatment with azole compounds. The results showed that the imidazole compounds (CTZ and KCZ) increased the protein expression of p53 (a maximal increase of 15-fold) and p27 (a maximal increase of 3.4-fold), in both breast cancer cell lines (Fig. 6B). However, treatment with CTZ increased p21 and p53 levels in MDA-MB-231 cells. The expression of CDK4, CDK2, and cyclin D1 proteins was inhibited by treatment with CTZ and KCZ in MDA-MB-231 cells. Moreover, a similar trend was also observed after the treatment of MCF-7 cells with azole compounds except cyclin D1 (Fig. 6B), where cyclin D1 level was considerably reduced by treatment with CTZ. There were no significant differences between triazole- and imidazole-treated both breast cancer cell lines in the expression of cyclin E1 (Fig. 6B).

In the mouse xenograft model, CTZ, KCZ, and ICZ inhibited tumor growth while FCZ did not (data not shown). CTZ, KCZ, and ICZ increased the expression of cleaved PARP in tissues derived from the xenograft tumor. In addition, p21 and p27 protein levels increased in xenograft tumor tissues derived from mice treated with imidazole (CTZ and KCZ) (Fig. 6C).

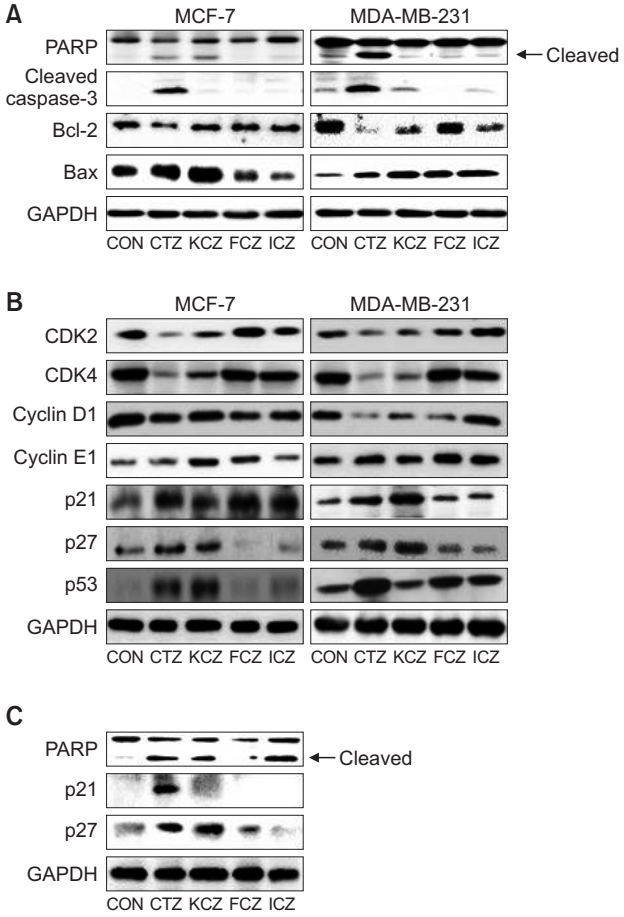

Fig. 6. Effect of azole antifungal compounds on protein expression. MCF-7 and MDA-MB-231 cells were treated with 50 μM imidazole [clotrimazole (CTZ) or ketoconazole (KCZ)] or triazole [fluconazole (FCZ) or itraconazole (ICZ)] compounds for 24 h. The protein expression related to apoptosis (A) and cell cycle (B) were examined in MCF-7 and MDA-MB-231 cells after treatment of each compound for 24 h. The protein expression was also examined in the xenograft model of MDA-MB-231 cells after treatment of each compound for 8 weeks (C). Glyceraldehyde 3-phosphate dehydrogenase (GAPDH) was used as the loading control. This experiment was performed three times. Band density was estimated using ImageJ 1.45s software (NIH).

Effects on cell invasion

We examined whether azole drugs could inhibit the invasiveness of cancer cells using a Matrigel-coated Boyden chamber. Fig. 7 shows that CTZ and KCZ significantly inhibited the invasiveness by 84.4% and 67.8%, respectively, in MDA-MB 231 cells. FCZ and ICZ did not significantly inhibit the invasiveness of MDA-MB-231 cells. However, there were no significant differences in invasiveness data for MCF-7 breast cancer cell lines after treatment with either imidazole or triazole compounds (data not shown).

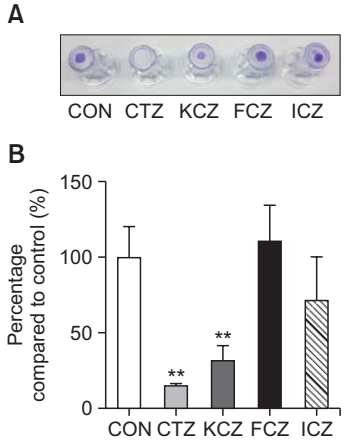

Fig. 7. Cell invasion assay of MDA-MB-231 cells (A). Quantification of the invasion density was measured by destaining the insert in methanol (B). Cells were treated with 50 μM imidazole [clotrimazole (CTZ) or ketoconazole (KCZ)] or triazole [fluconazole (FCZ) or itraconazole (ICZ)] compounds for 48 h. This experiment was performed three times and data are expressed as mean ± standard deviation (n=3). **p<0.01.

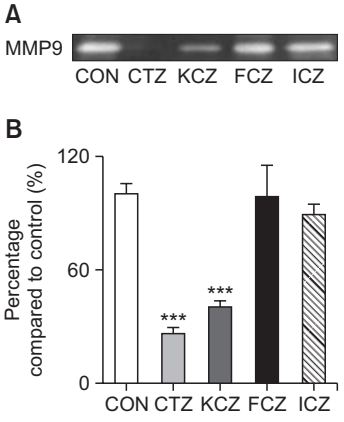

Fig. 8. Gelatin zymography of matrix metalloproteinase (MMP) 9. Gelatin zymography of concentrated conditioned medium from MDA-MB-231 cells treated with 50 μM imidazole [clotrimazole (CTZ) or ketoconazole (KCZ)] or triazole [fluconazole (FCZ) or itraconazole (ICZ)] compounds for 48 h (A). Quantification of MMP9 band density was analyzed using ImageJ 1.45s software (NIH) (B). This experiment was performed three times and data are expressed as mean ± standard deviation (n=3). ***p<0.001.

Gelatin zymography

MMP9 is known to be related to the degradation of the extracellular matrix (ECM) and plays a critical role in invasion and metastasis of tumors. Therefore, we examined whether azole compounds could inhibit the secretion of MMP9 from MCF-7 and MDA-MB-231 cells. Fig. 8 shows that the imidazole compounds (CTZ and KCZ) strongly inhibited the secretion of MMP9 from MDA-MB-231 cells by 74.0% and 59.3%, respectively, while the triazole compounds (FCZ and ICZ) did not. MMP9 was not secreted in MCF-7 cells and MMP2 was not detected in either MCF-7 or MDA-MB-231 cells (data not shown).

DISCUSSION

The traditional approach to the development of new drugs is both time-consuming and expensive and the success rate is very low. Therefore, we examined azole drugs, known as antifungal agents, to determine whether they have antitumor efficacy. This strategy is called drug repositioning, in which new indications are found for existing drugs (Shim and Liu, 2014). The use of established drugs can reduce the time and cost of development studies, and may increase the success rate (Shim and Liu, 2014; Tsubmoto *et al*., 2017).

In this study, we demonstrated that imidazole antifungal drugs (CTZ and KCZ) inhibited the proliferation of breast cancer cell lines. The triazole drug ICZ also inhibited the proliferation of MDA-MB-231 breast cancer cells but was not as effective as the imidazole drugs. Other researchers have reported the inhibition of cell viability by azole antifungal agents such as CTZ (Furtado *et al*., 2012, 2015), KCZ (Forgue-Lafitte *et al*., 1999), and ICZ (Pantziarka *et al*., 2015). The inhibition of cell proliferation caused by these agents was dose- and time-dependent. Other azole derivatives, metronidazole and secnidazole, which do not inhibit CYP-dependent enzymes, showed no growth inhibition of cancer cells (Maurice *et al*., 1992). Interestingly, in our study, FCZ, a CYP2C9 inhibitor, did not inhibit the proliferation of either breast cancer cell line. It has been reported that CTZ inhibits cell viability and cell proliferation by inducing glucose uptake in a dose-dependent manner and by decreasing intracellular ATP levels (Furtado *et al*., 2015). In this manner, CTZ inhibits the major enzymes involved in glycolysis, such as hexokinase, phosphofructokinase-1, and pyruvate kinase (Furtado *et al*., 2012, 2015). This is the probable mechanism for CTZ-induced inhibition of proliferation of breast cancer cells, especially of the highly metastatic cells, MDA-MB-231 (Furtado *et al*., 2012; Marcondes *et al*., 2015). However, the mechanism of action of CTZ has not been clearly explained.

Cancer cells affect various physiological changes through multiple pathways. Our data showed that the expression of the proteins p53 and p27 and the cleavage of the protein PARP increased in MCF-7 and MDA-MB-231 cells after treatment with CTZ and/or KCZ. A previous study reported that DNA damage-induced PARP cleavage increased p53 activity, which caused apoptosis (Ho *et al*., 1998; Ohnishi, 2005). That report indicated that imidazole compounds could induce apoptosis by inducing p53 levels and PARP cleavage in MCF-7 and MDA-MB-231 cells. Furthermore, the expression of CDK4, a cell cycle mitogen, decreased in MCF-7 and MDA-MB-231 cells after treatment with CTZ and/or KCZ (Bockstaele *et al*., 2006). Taken together, our data show that imidazole compounds are involved in multiple signaling pathways in breast cancer cells. Similarly, another study reported that imidazole compounds were anti-metabolites, and thus affected the suppression of cell growth and division (Baroniya *et al*., 2010).

Next, we focused on the invasiveness of breast cancer cells, since cancer cell metastasis is associated with cell migration and invasion (Hulkower and Herber, 2011). Our data showed that imidazole compounds suppressed the migratory and invasive ability of MDA-MB-231 breast cancer cells. CTZ and KCZ inhibited cell motility and invasion by inhibiting the secretion of MMP9 from MDA-MB-231 cells, which are the more aggressive cancer cells. MMP-mediated degradation of ECM is an important process in tumor invasion and metastasis

(Liao *et al*., 2012) and MMP9, in particular, might play a crucial role in tumor invasion and metastasis by damaging ECM (Yang *et al*., 2010; Gong *et al*., 2014).

Among the four azole antifungal drugs, the imidazole agents showed significantly stronger anticancer activity than the triazole agents. Generally, azole compounds, which inhibit CYP enzymes, have an antitumor effect (Zhang *et al*., 2011). The four antifungal drugs used in this study are all CYP inhibitors, especially of CYP2C and CYP3A, but the imidazole agents were more effective against the cancer cell lines than the triazole agents. Specifically, FCZ did not show any antitumor efficacy and ICZ had only a minimal effect on MDA-MB-231 cells. The mechanism of the anticancer effect for each compound is different. CTZ inhibits enzymes involved in the glycolytic process and KCZ inhibits arachidonic acid lipoxygenases and CYP enzymes. While ICZ only minimally inhibited cell proliferation in MDA-MB-231 cells, it has demonstrated antiangiogenic activity (Aftab *et al*., 2011) and inhibition of Hedgehog signaling in non-small cell lung carcinoma and in a primary non-small cell lung carcinoma xenograft model (Kim *et al*., 2010). So far, ICZ has been chosen for several clinical trials with cancer patients because triazole drugs are less toxic than imidazole compounds.

Taken together, we demonstrated the antitumor effects of imidazole compounds on cell proliferation, migration, and invasion in human breast cancer cell lines. Even though we did not investigate the specific pathways involved in the antitumor effects caused by imidazole drugs, they have well-established pharmacokinetic profiles and known toxicity, which can make these generic drugs strong candidates for repositioning as antitumor therapies. In future studies, we need to clarify the underlying mechanism of action and structure-activity relationship between imidazole and triazole compounds.

CONFLICT OF INTEREST

The authors declare that they have no conflicts of interest.

ACKNOWLEDGMENTS

This research was supported by the Basic Science Research Program through the National Research Foundation of Korea (NRF) funded by the Ministry of Science, ICT and Future Planning (NRF-2015R1A2A2A01007546 and NRF-2018R1A2B6004895) and the Korea Health Technology R&D Project (HI16C0992) through the Korea Health Industry Development Institute (KHIDI) funded by the Ministry of Health & Welfare, Republic of Korea.

REFERENCES

Aftab, B. T., Dobromilskaya, I., Liu, J. O. and Rudin, C. M. (2011) Itraconazole inhibits angiogenesis and tumor growth in non-small cell lung cancer. *Cancer Res.* **71**, 6764-6772.

Antonarakis, E. S., Heath, E. I., Smith, D. C., Rathkopf, D., Blackford, A. L., Danila, D. C., King, S., Frost, A., Ajiboye, A. S., Zhao, M., Mendonca, J., Kachhap, S. K., Rudek, M. A. and Carducci, M. A. (2013) Repurposing itraconazole as a treatment for advanced prostate cancer: a noncomparative randomized phase II trial in men with metastatic castration-resistant prostate cancer. *Oncologist* **18**, 163-173.

Baroniya, S., Anwer, Z., Sharma, P. K., Dudhe, R. and Kumar, N. (2010) Recent advancement in imidazole as anticancer agents: a review. *Der Pharmacia Sinica* **1**, 172-182.

Bockstaele, L., Coulonval, K., Kooken, H., Paternot, S. and Roger, P. P. (2006) Regulation of CDK4. *Cell Div.* **1**, 25.

Bray, F., Ren, J. S., Masuyer, E. and Ferlay, J. (2013) Global estimates of cancer prevalence for 27 sites in the adult population in 2008. *Int. J. Cancer* **132**, 1133-1145.

Cook, K. L., Shajahan, A. N., Warri, A., Jin, L., Hilakivi-Clarke. L. A. and Clarke, R. (2012) Glucose-regulated protein 78 controls cross-talk between apoptosis and autophagy to determine antiestrogen responsiveness. *Cancer Res.* **72**, 3337-3349.

Ferlay, J., Soerjomataram, I., Ervik, M., Dikshit, R., Eser, S., Mathers, C., Rebelo, M., Parkin, D. M., Forman, D. and Bray, F. (2013) GLOBOCAN 2012 v1.0, Cancer Incidence and Mortality Worldwide: IARC CancerBase No. 11. International Agency for Research on Cancer, Lyon, France. Available from: http://globocan.iarc.fr/.

Forgue-Lafitte, M. E., Coudray, A. M., Fagot, D. and Mester, J. (1999) Effects of ketoconazole on the proliferation and cell cycle of human cell lines. *Cancer Res.* **52**, 827-6831.

Fujita, Y., Kimura, M., Sato, H., Takata, T., Ono, N. and Nishio, K. (2016) Characterization of the cytotoxic activity of [2]rotaxane (TRO-A0001), a novel supramolecular compound, in cancer cells. *Arch. Pharm. Res.* **39**, 825-832.

Furtado, C. M., Marcondes, M. C., Sola-Penna, M., de Souza, M. L. and Zancan, P. (2012) Clotrimazole preferentially inhibits human breast cancer cell proliferation, viability and glycolysis. *PLoS ONE* **7**, e30462.

Furtado, C. M., Marcondes, M. C., Carvalho, R. S., Sola-Penna, M. and Zancan, P. (2015) Phosphatidylinositol-3-kinase as a putative target for anticancer action of clotrimazole. *Int. J. Biochem. Cell Biol.* **62**, 132-141.

Gong, Y., Chippada-Venkata, U. D. and Oh, W. K. (2014) Roles of matrix metalloproteinases and their natural inhibitors in prostate cancer progression. *Cancers (Basel)* **6**, 1298-1327.

Ho, Y. S., Tsai, P. W., Yu, C. F., Liu, H. L., Chen, R. J. and Lin, J. K. (1998) Ketoconazole-induced apoptosis through p53-dependent pathway in human colorectal and hepatocellular carcinoma cell lines. *Toxicol. Appl. Pharmacol.* **153**, 39-47.

Hulkower, K. I. and Herber, R. L. (2011) Cell migration and invasion assays as tools for drug discovery. *Pharmaceutics* **3**, 107-124.

Kadavakollu, S., Stailey, C., Kunapareddy, C. S. and White, S. (2014) Clotrimazole as a cancer drug: a short review. *Med. Chem.* **4**, 722-724.

Kim, J., Tang, J. Y., Gong, R., Kim, J., Lee, J. J., Clemons, K. V., Chong, C. R., Chang, K. S., Fereshteh, M., Gardner, D., Reya, T., Liu, J. O., Epstein, E. H., Stevens, D. A. and Beachy, P. A. (2010) Itraconazole, a commonly used antifungal that inhibits Hedgehog pathway activity and cancer growth. *Cancer Cell* **17**, 388-399.

Li, D. H., Hu, P., Xu, S. T., Fang, C. Y., Tang, S., Wang, X. Y., Sun, X. Y., Li, H., Xu, Y., Gu, X. K. and Xu, J. Y. (2017) Lasiokaurin derivatives: synthesis, antimicrobial and antitumor biological evaluation, and apoptosis-inducing effects. *Arch. Pharm. Res.* **40**, 796-806.

Liao, C. L., Lai, K. C., Huang, A. C., Yang, J. S., Lin, J. J., Wu, S. H., Gibson Wood, W., Lin, J. G. and Chung, J. G. (2012) Gallic acid inhibits migration and invasion in human osteosarcoma U-2 OS cells through suppressing the matrix metalloproteinase-2/-9, protein kinase B (PKB) and PKC signaling pathways. *Food Chem. Toxicol.* **50**, 1734-1740.

Lim, S. J., Choi, H. G., Jeon, C. K. and Kim, S. H. (2015) Increased chemoresistance to paclitaxel in the MCF10AT series of human breast epithelial cancer cells. *Oncol. Rep.* **33**, 2023-2030.

Mander, S., You, D. J., Park, S., Kim, D. H., Yong, H. J., Kim, D. S., Ahn, C., Kim, Y. H., Seong, J. Y. and Hwang, J. I. (2018) Nafamostat mesilate negatively regulates the metastasis of triple-negative breast cancer cells. *Arch. Pharm. Res.* **41**, 229-242.

Marcondes, M. C., Fernandes, A. C., Itabaiana, I., Jr., de Souza, R. O., Sola-Penna, M. and Zancan, P. (2015) Nanomicellar formulation of clotrimazole improves its antitumor action toward human breast cancer cells. *PLoS ONE* **10**, e0130555.

Maurice, M., Pichard, L., Daujat, M., Fabre, I., Joyeux, H., Domergue,

J. and Maurel, P. (1992) Effects of imidazole derivatives on cytochrome P-450 from human hepatocytes in primary culture. *FASEB J.* **6**, 752-758.
Ohnishi, T. (2005) The role of the p53 molecule in cancer therapies with radiation and/or hyperthermia. *J. Cancer Res. Ther.* **1**, 147-150.
Pantziarka, P., Sukhatme, V., Bouche, G., Meheus, L. and Sukhatme, V. P. (2015) Repurposing drugs in oncology (ReDO)-itraconazole as an anti-cancer agent. *Ecancermedicalscience* **9**, 521.
Shim, J. S. and Liu, J. O. (2014) Recent advances in drug repositioning for the discovery of new anticancer drugs. *Int. J. Biol. Sci.* **10**, 654-663.
Steeg, P. S. (2006) Tumor metastasis: mechanistic insights and clinical challenges. *Nat. Med.* **12**, 895-904.
Taplin, M. E., Regan, M. M., Ko, Y. J., Bubley, G. J., Duggan, S. E., Werner, L., Beer, T. M., Ryan, C. W., Mathew, P., Tu, S. M., Denmeade, S. R., Oh, W. K., Sartor, O., Mantzoros, C. S., Rittmaster, R., Kantoff, P. W. and Balk, S. P. (2009) Phase II study of androgen synthesis inhibition with ketoconazole, hydrocortisone, and dutasteride in asymptomatic castration-resistant prostate cancer. *Clin. Cancer Res.* **15**, 7099-7105.
Tran, B. N., Nguyen, H. T., Kim, J. O., Yong, C. S. and Nguyen, C. N. (2017) Combination of a chemopreventive agent and paclitaxel in CD44-targeted hybrid nanoparticles for breast cancer treatment. *Arch. Pharm. Res.* **40**, 1420-1432.
Tripathi, K. D. (2013) Essentials of Medical Pharmacology, 7th ed, p. 791. JP Medical Ltd, London.
Tsubamoto, H., Ueda, T., Inoue, K., Sakata, K., Shibahara, H. and Sonoda, T. (2017) Repurposing itraconazole as an anticancer agent. *Oncol. Lett.* **14**, 1240-1246.
Vasaitis, T. S., Bruno, R. D. and Njar, V. C. (2011) CYP17 inhibitors for prostate cancer therapy. *J. Steroid Biochem. Mol. Biol.* **125**, 23-31.
Yang, S. F., Chen, M. K., Hsieh, Y. S., Yang, J. S., Zavras, A. I., Hsieh, Y. H., Su, S. C., Kao, T. Y., Chen, P. N. and Chu, S. C. (2010) Antimetastatic effects of Terminalia catappa L. on oral cancer via a down-regulation of metastasis-associated proteases. *Food Chem. Toxicol.* **48**, 1052-1058.
Zhang, R., Pan, X., Huang, Z., Weber, G. F. and Zhang, G. (2011) Osteopontin enhances the expression and activity of MMP-2 via the SDF-1/CXCR4 axis in hepatocellular carcinoma cell lines. *PLoS ONE* **6**, e23831.
Zhao, H. G., Zhou, S. L., Lin, Y. Y., Dai, H. F. and Huang, F. Y. (2018) Toxicarioside N induces apoptosis in human gastric cancer SGC-7901 cell by activating the p38MAPK pathway. *Arch. Pharm. Res.* **41**, 71-78.